11th International Symposium on Magnetic Bearings
August 26-29, Nara, Japan

A PHASE MODULATION SELF-SENSING TECHNOLOGY OF ACTIVE MAGNETIC BEARINGS USING A HIGH FREQUENCY VOLTAGE INJECTION METHOD

Young Ho Park
School of Mechanical & Aerospace Eng., Seoul National Univ., Seoul 151-742 Korea
reservoir9@amed.snu.ac.kr
In Hwang Park
BK21 School for Creative Eng. Design of Next Gen. Mech. & Aero. Sys., Seoul 151-742 Korea
zeus@amed.snu.ac.kr
Hee Doh Jang
School of Mechanical & Aerospace Eng., Seoul National Univ., Seoul 151-742 Korea
nismo1004@amed.snu.ac.kr
Dong Chul Han
School of Mechanical & Aerospace Eng., Seoul National Univ., Seoul 151-742 Korea
dchan@amed.snu.ac.kr

ABSTRACT

Conventional AMBs (active magnetic bearings) systems consist of electromagnetic coils, position sensors, power amplifiers and a feedback controller. This hardware configuration can lead to a structural complexity, problems of space limitations for the installation. In this paper, a self-sensing mechanism is proposed to resolve such limitations of the general AMB system. The proposed self-sensing scheme uses a phase difference of the injected current of two opposite electromagnetic actuators while an object levitating between the actuators. The relationship between the phase difference of injected currents and the position of a levitated object was theoretically derived and linearized. In order to realize the proposed self-sensing scheme, a signal processing algorithm was developed. The frequency response of the estimator was measured to verify the performance of the proposed self-sensing scheme. In addition, a magnetic levitation and a disturbance rejection response were experimentally obtained to verify the feasibility of the proposed self-sensing mechanism. Experimental results showed that the developed self-sensing technique has similar performance as a practical gap sensor.

1 INTRODUCTION

In recent decades, AMBs have been widely used due to their unique advantages such as non-contact, lubrication-free support and controllability of actuator characteristics in many industrial machines. By virtue of such merits, AMB has become an essential machine element of high-speed rotating machinery, including turbo molecular pumps and high-speed machining centers. The need for AMBs has been also increasing

in non-traditional application areas where compact size is required. For example, small-sized AMBs can be applied to portable hard disk drive systems, artificial heart blood pumps and audio loudspeakers.

There have been two approaches to realize the self-sensing technology for AMB systems. One is to use a state model. In this approach, the object position can be estimated by constructing state observer and measuring the electromagnetic coil current. This was first studied by Visher et al. [1]. However, due to poor observability at high frequency [2], detailed modeling and considerations for changes of environments are necessary. The other approach is to use a high frequency carrier using PWM (pulse width modulation) power amplifiers which drive the electromagnetic coils. Since the current ripples generated by PWM carrier component are related to inductance variation, the object position can be estimated by measuring the high frequency current ripple. This was suggested by Okada et al. **[3]**. However, since the current ripples corresponding to PWM carrier frequency may also be changed by duty ratio, it is necessary to take the duty ratio into the consideration for the controller design by measuring voltage ripples [4, 5, 12] or using a nonlinear observer [6, 7, 11]. For improved position accuracy, magnetic material permeability can be compensated using an approximated static permeability curve [8, 10].

Although several self-sensing technologies have been proposed for years, applying such technologies for industrial applications still remain a challenging problem. To improve the performance of conventional self-sensing technologies and to make the technology more applicable to industrial applications, a self-sensing scheme using a phase modulation algorithm based on a high frequency voltage injection method is proposed. Unlike the other self-sensing technologies [3 – 12], the proposed technology doesn't need any compensations including duty ratio. In addition, since white noises generally have not a phase information but an amplitude information, the proposed method may be robust to noise over other technologies.

This paper will begin with a theory of the proposed self-sensing mechanism, followed by a signal processing algorithm for the self-sensing scheme (section 2). Finally, frequency response of the proposed estimation algorithm is experimentally measured to evaluate the dynamic performance. The self-sensing signal is compared to a reference eddy current sensor signal when a one degree-of-freedom mechanical system is magnetically levitated and disturbance is rejected (section 3).

2 PHASE MODULATION SELF-SENSING AMB

2.1 Scheme

Figure 1 shows the proposed self-sensing AMB system scheme. This system is composed of a pair of electromagnetic actuators (EMA1 and EMA2), PWM power amplifiers, current controllers, a position controller and a position estimator. A conventional AMB system has a position sensor (e.g., eddy-current, inductive or capacitive position sensor) which causes hardware complexity and installation problem. But the proposed system uses the position estimator instead of a position sensor. This scheme can resolve the limitation caused by a position sensor of the conventional AMB system.

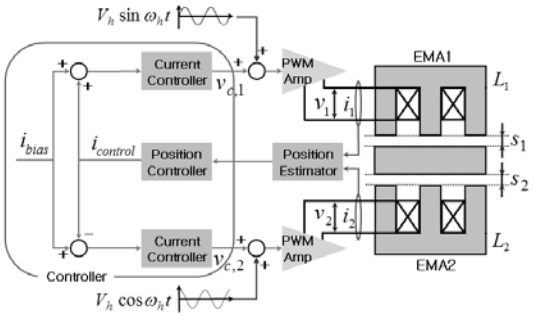

FIGURE 1 The proposed self-sensing AMB

The object moves along the s_1 or s_2 direction. If the core loss and the coil capacitance can be negligible, the voltage v and the current i of the EMA have the following relationship.

$$v = R \cdot i + L\frac{di}{dt} \tag{1}$$

In addition to the voltage signals v_{c1}, v_{c2} to control the EMA currents, the high-frequency sinusoidal waveforms $V_h \sin \omega_h t$, $V_h \cos \omega_h t$ for self-sensing estimation are applied to the EMAs as shown in figure 1. If the injection frequency ω_h is much higher than the frequency bandwidth to control the EMA currents, the ω_h components in equation (1) can be considered alone. Then, the amplitude and the phase of the EMA currents corresponding to ω_h can be obtained as given in equation (2). For simplicity, the EMA1 where the sine waveform is injected is considered.

$$i = I_h \sin(\omega_h t + \phi) \tag{2}$$

where $I_h = \dfrac{V_h}{\sqrt{R^2 + (\omega_h L)^2}}, \tan\phi = -\dfrac{\omega_h L}{R}$

The inductance L of the EMA is a function of coil turn number n, cross-sectional area A of magnetic flux passage, magnetic permeability μ_0 in vacuum, and gap distance s between the EMA and the levitated object [9].

$$L = \frac{\mu_0 n^2 A}{2s} \tag{3}$$

From equations (2) and (3), the change in the gap distance causes the change in the inductance, resulting in the change of EMA current amplitude and phase. In this paper, the change of the EMA current phase will be used to estimate the change of the gap distance. Since the relationship between ϕ and s in equations (2) and (3) is nonlinear, it is difficult to implement ϕ - s relationship while applying a position control algorithm. Thus, the ϕ - s relationship needs linearization at operating points. For linearization, it is assumed that the moving distance of the levitated object is very small from the operating point. Then, s, L and ϕ can be expressed as following.

$$s = s_0 + \Delta s \tag{4}$$

$$L = L_0 + \Delta L \tag{5}$$

$$\phi = \phi_0 + \Delta\phi \tag{6}$$

where subscript 0 and Δ denote the operating point and small deviations respectively.

To linearize $\Delta\phi - \Delta s$ relationship, $\Delta L - \Delta s$ and $\Delta\phi - \Delta L$ linear relationships are utilized because $\Delta\phi - \Delta s$ linear relationship cannot be obtained directly.

Substituting s in equation (4) into s in equation (3) and using the Taylor series expansion at s_0, the resulting inductance L is modified as following.

$$\begin{aligned} L &= \frac{\mu_0 n^2 A}{2}\left(\frac{1}{s_0 + \Delta s}\right) \\ &\approx \frac{\mu_0 n^2 A}{2s_0}\left(1 - \frac{\Delta s}{s_0}\right) \\ &= L_0\left(1 - \frac{\Delta s}{s_0}\right) \end{aligned} \tag{7}$$

where $L_0 = \dfrac{\mu_0 n^2 A}{2s_0}$.

Comparing the equations (5) and (7), ΔL is expressed as following.

$$\Delta L = -\frac{L_0}{s_0}\Delta s \tag{8}$$

So, the linear relationship between ΔL and Δs is acquired as shown in equation (8).

Now, to get $\Delta\phi - \Delta L$ linear relationship, let us substitute ϕ in equation (6) into ϕ in equation (2). Then we can obtain,

$$\begin{aligned}\tan\phi &= \tan(\phi_0 + \Delta\phi) \\ &= -\frac{\omega_h \cdot (L_0 + \Delta L)}{R} \\ &= \tan\phi_0 - \frac{\omega_h \cdot \Delta L}{R}\end{aligned} \tag{9}$$

where $\tan\phi_0 = -\frac{\omega_h \cdot L_0}{R}$.

On the other hand, $\tan\phi$ in equation (2) can be rewritten using the Taylor series expansion at ϕ_0.

$$\tan\phi = \tan\phi_0 + \Delta\phi \sec^2\phi_0 \tag{10}$$

Comparing the equations (9) and (10), $\Delta\phi - \Delta L$ relationship can be obtained.

$$\begin{aligned}\Delta\phi &= -\frac{1}{\sec^2\phi_0} \cdot \frac{\omega_h \cdot \Delta L}{R} \\ &= -\frac{\omega_h R}{R^2 + (\omega_h L_0)^2}\Delta L\end{aligned} \tag{11}$$

where $\sec\phi_0 = \sqrt{R^2 + (\omega_h \cdot L_0)^2} / R$.

Consequently, $\Delta s - \Delta\phi$ linear relationship is obtained from equations (8) and (11) as given in equation (12).

$$\Delta s = \frac{s_0 \omega_h L_0}{R}\Delta\phi; \quad (\omega_h \cdot L_0 >> R) \tag{12}$$

Since the position change Δs is linearly dependent on the phase change $\Delta\phi$, the position s can be estimated by measuring the coil current phase change $\Delta\phi$, multiplying $\Delta\phi$ by $\frac{s_0 \omega_h L_0}{R}$ which is constant under a specific system and adding the operating position s_0.

2.2 Signal processing method

In general, conventional EMAs can be controlled by feedback of the opposite position difference $s_1 - s_2$, shown in Figure 1. However, as stated in equation (12), the proposed self-sensing EMAs can be controlled by the current phase difference $\phi_1 - \phi_2$ instead of the position difference $s_1 - s_2$. In order to get the phase difference, a trigonometric conversion formula that converts multiplication into sum is used. When the trigonometric conversion formula is used, the phase difference of injection signals should be $\pi/2$. This is because the phase difference of two injection signals can be approximately acquired by using the sinusoidal functions. For instance, when multiplication of two sinusoidal functions with same phase is converted into sum using the trigonometric conversion formula, it is expressed by sum of two cosine function. Therefore, if the phase difference of two injection signals is very small, the corresponding cosine value of the phase difference is nearly 0; hence, the phase difference cannot be obtained approximately. On the other hand, when multiplication of two sinusoidal functions with $\pi/2$ phase difference is converted into sum, it is expressed by sum of two sine function. Therefore, with the small phase difference, the corresponding sine value of the phase difference can be approximated to the value of phase difference.

From equation (2), The currents of two EMAs can be expressed as following if $\omega_h \cdot L >> R$.

$$i_1 = \frac{V_h}{\omega_h L_1}\sin(\omega_h t + \phi_1) \tag{13}$$

$$i_2 = \frac{V_h}{\omega_h L_2}\cos(\omega_h t + \phi_2) \tag{14}$$

Then the multiplication of the currents can be written as,

$$i_1 i_2 = \frac{V_h^2}{2\omega_h^2 L_1 L_2}\left\{\sin\left(2\omega_h t + \phi_1 + \phi_2\right) + \sin\left(\phi_1 - \phi_2\right)\right\} \tag{15}$$

To remove a doubled high frequency term, a low-pass filter is adopted. Thus the multiplication of the two currents after the low-pass filter can be obtained approximately as following.

$$LPF\left(i_1 i_2\right) \approx \frac{1}{2}\left(\frac{V_h}{\omega_h L_0}\right)^2 \left(\phi_1 - \phi_2\right) \tag{16}$$

Since $\sin\left(\phi_1 - \phi_2\right) \approx \phi_1 - \phi_2$ and $L_1 L_2 = \left(L_0^2 - \Delta L^2\right) \approx L_0^2$ at operating point, the resulting position difference is estimated by substituting the phase difference in equation (16) into equation (12). Consequently, we can obtain the final relationship between the phase difference of the injected currents and the position difference of the 2 EMAs as following.

$$\frac{1}{2}\left(s_1 - s_2\right) = \frac{s_0 \omega_h^3 L_0^3}{R V_h^2} \cdot LPF\left(i_1 i_2\right) \tag{17}$$

Figure 2 shows the signal processing block diagram.

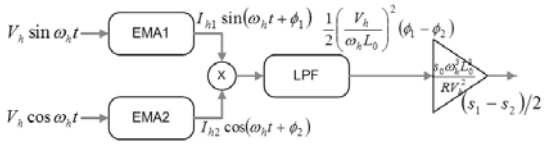

FIGURE 2 Signal processing block diagram

3 EXPERIMENTS

The frequency response of the position estimator is necessary to verify the performance of the proposed self-sensing technology. A test rig was designed and constructed to get the frequency response as shown in Figure 3. This test rig is composed of a cantilever, two EMAs and two conventional eddy-current gap sensors. The cantilever was installed at the center between two EMAs. The gap sensors were installed as close as possible to the EMAs. The EMAs were controlled with a digital signal processor (TI Inc., TMS320F2812) and PWM power amplifiers were made with smart power module (Fairchild Inc., FSAM10SH60A). The reference gap sensor was an eddy-current sensor (KAMAN Inc., KD23001SUM). Table 1 shows the specifications of EMAs.

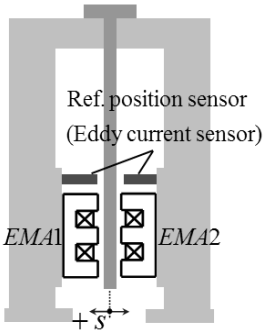

FIGURE 3 Cantilever test rig for EMA performance

TABLE 1 EMA specifications

Nominal air gap	0.3mm
Number of turns of each coil	152
Cross sectional area of air gap	166.6mm^2
Nominal inductance	0.0136H
Resistance	1.5Ω
Switching frequency	12kHz
Injection frequency	3.0kHz
Magnitude of injection voltage	10V
DC link voltage	45V

The frequency response of position estimator was measured as following.

1) The cantilever was excited by two EMAs

where the chirp signal generated by a dynamic signal analyzer (HP Inc., 25670A) was injected.

2) The output signals of the gap sensor and the position estimator were measured.

3) Consequently, the frequency response of the estimator was measured by the ratio of output signal of gap sensor to that of estimator.

Figure 4 shows the frequency response of the estimator showing bandwidth of about 50Hz.

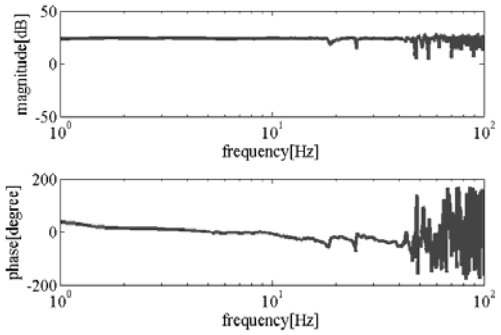

FIGURE 4 Frequency response of the position estimator

To verify the feasibility of the proposed self-sensing mechanism, a one degree-of-freedom mechanical system was designed. As shown in Figure 5, a mass center of a rolling mass was on a pivot point so that the rolling mass can only rotate around its center of mass. The EMAs are installed at both ends of the rolling mass to control the rotating motion of the rolling mass. Practical gap sensors (KAMAN Inc., KD23001SUM) were installed as close as possible to the EMAs. The controller and power amplifiers were same as those used previously in the cantilever test rig. The current controller uses a PI control algorithm to control the EMA currents with 300Hz cutoff frequency and the position controller uses a PD control algorithm to control the rolling mass position.

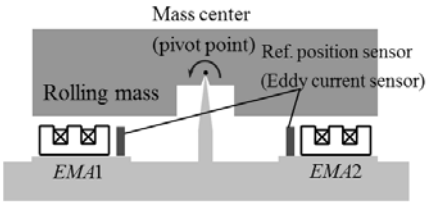

FIGURE 5 One D.O.F. mechanical system for feasibility test of the proposed self-sensing theory

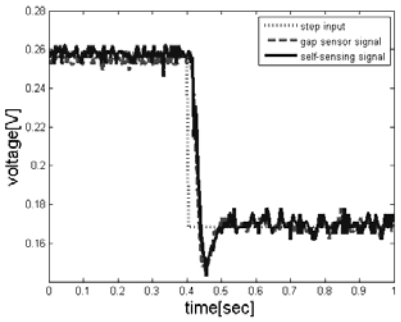

FIGURE 6 Magnetic levitation response

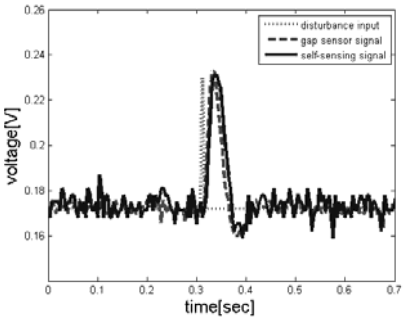

FIGURE 7 Disturbance rejection response

Figure 6 and 7 show a magnetic levitation and a disturbance rejection response, respectively. It can be seen that the levitated object was stably suspended and the disturbance was rejected. These results also show that the self-sensing signal is consistent with the signal

from the gap sensor signal. Therefore, it is confirmed that the proposed self-sensing mechanism can be used to both estimate the position of an object and to control the object suspension. As a result, the removal of a position sensor will decrease structural complexity and installation space.

4 CONCLUSIONS

This paper proposes a developed self-sensing technology to make it more practicable. The proposed mechanism using the phase modulation algorithm is based on the high frequency voltage injection method with a PWM power amplifier. And the position estimator worked without any compensation about duty ratio changes.

The relationship between the phase change and the levitated object position was theoretically derived and linearized to implement easily. And this relationship was compensated after measured EMA inductance value with LCR meter had been compared to theoretical value. As a result, the modification constant K was discovered experimentally.

To verify the performance of the proposed self-sensing technology, the frequency response of the position estimator was measured through the cantilever test rig. The estimator showed a bandwidth of about 50Hz.

Finally, to verify the feasibility, the magnetic levitation and the disturbance rejection response were obtained through a one degree-of-freedom mechanical system. The results demonstrate that the proposed self-sensing technology shows same performance as a practical position sensor.

ACKNOWLEDGEMENT

This work was supported by the second stage of the Brain Korea 21 Project in 2007 and Ministry of Science & Technology and special thanks is given to the Institute of Advanced Machinery and Design at Seoul National University.

REFERENCES

1. D. Vischer, Sensorlose und spannungsgesteuerte magnetlager, Ph.D. dissertation, Dept. Mech. Eng., Swiss Federal Inst. Technol., (1988) no. 8665.

2. L. Kuˇcera, Robustness of self-sensing magnetic bearings, in Proc. Magnetic Bearings Industrial Conf., (1997) 261–270.

3. Y. Okada, K. Matsuda, and B. Nagai, Sensorless magnetic levitation control by measuring the PWM carrier frequency component, in Proc. 3rd Int. Symp. Magnetic Bearings, (1992) 176–183.

4. V. Iannello, Sensorless Position for an Active Magnetic Bearing. U. S. Patent 5 696 412, (1997).

5. N. Skricka and R. Markert, Compensation of disturbances on self-sensing magnetic bearings caused by saturation and coordinate coupling, in Proc. 7th Int. Symp. Magnetic Bearings. (2000) 165–170.

6. M. D. Noh and E. H. Maslen, Position estimation in magnetic bearings using inductance measurements, in Proc. Magnetic Bearings Industrial Conf., (1995) 249–256.

7. D. T. Montie and E. H. Maslen, Experimental self-sensing results for a magnetic bearing, in Proc. 7th Int. Symp. Magnetic Bearings. (2000) 171–176.

8. A. Schammass, A self-sensing active magnetic bearing: Modulation approach, Ph.D. dissertation, EPF, Lausanne, (2003) no. 2841.

9. G. Schweitzer, H. Bleuler, A. Traxler, Active Magnetic Bearings: Basics, Properties and Applications of Active Magnetic Bearings, vdf

Houchschulverlag AG der ETH Zurich, (1994).
10. A. Schammass, R. Herzog, P. Bühler, and H. Bleuler, New Results for Self-Sensing Active Magnetic Bearings Using Modulation Approach, IEEE Transactions on Control Systems Technology, vol. 13, no.4, july (2005) 509-516.
11. K. S. Peterson, R. H. Middleton and J. S. Freudenberg, Fundamental Limitations in Self-Sensing Magnetic Bearings when Modeled as Linear Periodic Systems, Proceedings of the 2006 American Control Conference Minneapolis, Minnesota, USA, June 14-16, (2006) 4552-4557